

## A Methodology for Fast and Accurate Analytical Fragility Analysis of Linear Structural Systems during Wind Storms: ALFA

Cihan Çiftci\*<sup>1</sup> 

\*<sup>1</sup> Abdullah Gul University, Faculty of Engineering, Department of Civil Engineering, KAYSERİ, TURKEY

(Alınış / Received: 09.08.2023, Kabul / Accepted: 27.12.2023, Online Yayınlanma / Published Online: 30.12.2023)

### Keywords

Fragility Curve,  
Monte-Carlo Simulation,  
Wind Force,  
Structural Reliability,  
Structural Dynamics

**Abstract:** Wind-storms are extremely destructive natural disasters that cause structural damage, and consequently severe personal injuries and casualties. To reduce these injuries and casualties, risk assessment of existing structures and improvement of building design regulations have become important. To assess the risk of structural systems, analytical fragility analysis is a recently developed method by providing conditional failure probabilities for the structural systems. However, the analytical fragility analysis requires extensive computational time and effort which makes it infeasible for large scale structures. This proposed paper develops a new methodology (Analytical Linear Fragility Analysis: ALFA) to simplify and to expedite the analytical fragility analysis for linear structural systems without compromising accuracy. ALFA is exemplified by obtaining the fragility curves of 70 different multi-degree of freedom linear mass-column systems subjected to varying wind loading conditions. The fragility curves of the same mass-column systems were also obtained using Monte-Carlo (MC) based brute-force methodology, which is a commonly used computationally expensive method in literature, and results are compared. This comparison yields the conclusion that ALFA is 240 times faster than the brute-force one, without losing accuracy. Moreover, ALFA can be utilized for improvement of performance-based design specifications and the preliminary risk assessment of nonlinear structural systems.

## Rüzgar Fırtınaları Sırasında Lineer Yapısal Sistemlerin Hızlı ve Doğru Analitik Kırılabilirlik Analizi için Bir Metodoloji: ALFA

### Anahtar Kelimeler

Kırılabilirlik Eğrisi,  
Monte-Carlo Simülasyonu,  
Rüzgar Yüğü,  
Yapısal Güvenilirlik,  
Yapısal Dinamik

**Öz:** Rüzgar fırtınaları, yapısal hasara ve sonuç olarak ciddi kişisel yaralanmalara ve kayıplara neden olan son derece yıkıcı doğal afetlerdir. Bu yaralanma ve can kayıplarını azaltmak için mevcut yapıların risk değerlendirmesi ve bina tasarım yönetmeliklerinin iyileştirilmesi önem kazanmıştır. Yapısal sistemlerin riskini değerlendirmek için, analitik kırılabilirlik analizi, yapısal sistemler için koşullu arıza olasılıkları sağlayarak son zamanlarda geliştirilen bir yöntemdir. Bununla birlikte, analitik kırılabilirlik analizi, büyük ölçekli yapılar için uygulanamaz hale getiren kapsamlı hesaplama zamanı ve çabası gerektirir. Önerilen bu makale, doğruluktan ödün vermeden doğrusal yapısal sistemler için analitik kırılabilirlik analizini basitleştirmek ve hızlandırmak için yeni bir metodoloji (Analitik Lineer Kırılabilirlik Analizi: ALFA) geliştirmektedir. ALFA, değişen rüzgar yükü koşullarına maruz kalan 70 farklı çok serbestlik dereceli lineer kütle kolon sisteminin kırılabilirlik eğrilerinin elde edilmesiyle örneklenmiştir. Literatürde hesaplama açısından pahalı bir yöntem olan Monte-Carlo (MC) tabanlı kaba-kuvvet metodolojisi kullanılarak aynı kütle-kolon sistemlerinin kırılabilirlik eğrileri elde edilmiş ve sonuçlar karşılaştırılmıştır. Bu karşılaştırma, ALFA'nın kesinliği kaybetmeden kaba kuvvetten 240 kat daha hızlı olduğu sonucunu verir. ALFA, performans dayalı tasarımların iyileştirilmesi ve doğrusal olmayan yapısal sistemlerin ön risk değerlendirmesi için kullanılabilir.

\*Corresponding Author, email: cihan.ciftci@agu.edu.tr

## 1. Introduction

Bu Wind-storms (hurricanes, typhoons, and tropical cyclones) can be accepted to be one of the most devastating and costly natural disasters affecting civil infrastructures [1–6], live trees in forest and urban areas [7,8], and consequently human lives. These natural disasters cause significant property damages and personal injuries – even fatally [4,9,10]. For instance, two different tornadoes in 2011, which cut through Tuscaloosa, Alabama and Joplin, Missouri, caused a total of 553 recorded fatalities [11]. Furthermore, wind-induced tree failures cause an average of 31 deaths per year in the United States, according to the records during 1995-2007 [10]. Thus, arborists, structural engineers, insurance industries, and regulatory authorities (e.g., NIST, IBHS, FEMA, ASCE, AISC, and ACI) greatly exert to mitigate these human and socio-economic losses by providing advanced risk assessment of structures and also by improving the current building design specifications and guidelines [1,4,7–9,12]. For the advanced risk assessment of constructions (e.g., [2,13–16]) and live trees (e.g., [8]), analytical fragility analysis is recently adopted tool to construct the fragility curves of the structures.

Analytical fragility analysis, which is introduced in the early 1980s for the risk assessment of nuclear power plants (e.g., [17–19]), is a tool to provide conditional failure probabilities of structural systems. The fragility analysis has been received increasing attention among scientific community studying on performance-based structural engineering since, especially, last two decades [20]. Recently, fragility analysis is a preferable tool used by researchers on wind (e.g., [2,8,13–16,21–23]) or seismic loading (e.g., [20,24–27]) for the risk assessment of structures. In regard to the wind loading, the studies of Ellingwood et al. [22], Lee and Rosowsky [13], van de Lindt and Dao [14], Quilligan et al. [15], Ciftci et al. [8], and Sim and Jung [16] addressed the fragility analysis for light-frame wood failures, roof sheathing failures, wood-frame building failures, steel and concrete wind turbine towers, live-tree failures, and window failures in buildings, respectively.

For the analytical fragility analysis of structures, Monte-Carlo (MC) Simulation is the most commonly used reliable method by researchers to randomly generate sampling data [8,16,28]. Using the MC simulations, the risk assessment of structures can be done by considering the effects of several uncertainties, involved either in the mechanical and physical properties of the structures or in the loading condition exerted on the structures. It is difficult to develop an analytical closed-form formulas or explicit equations for a relationship between these uncertainties and the dynamic response of the structures [24]; thus all these uncertainties can be combined into MC simulations (as a brute-force approach) to represent the combined effects of the uncertainties on the risk assessment of structures and to statistically construct accurate and reliable fragility curves. However, the main disadvantage of the MC simulations is to be greatly computationally expensive [29,30]. Randomly generated sampling data of MC simulations are delivered to an external finite element (FE) based package-program that requires extensive computational time and effort to accurately calculate demand stresses or deformations of the structures using full dynamic time history analyses [31]. In order to reduce these extensive computational time and effort, the analytical fragility analysis traditionally utilizes an empirical method, which is called as two-parameter lognormal distribution function, originally developed in 1980s [31]. This method is based on a statistical relationship between external loading parameters (e.g., wind speed, peak ground acceleration-PGA, and spectrum intensity-SI) and the dynamic response of structures. Thus, the analytical fragility curves of structures are traditionally constructed to be a lognormal cumulative distribution function based on this relation, which can be obtained using a less number of FE based MC simulations [2,13,16,18,26,32–34]. However, this method may have non-negligible errors due to the dispersions in the statistical relationship between external loading parameters and the dynamic response of structures [35]. Also, Jeong and Elnashai presented a new simplification method to reduce the extensive computational time and effort for the construction of fragility curves [31]. In this study, first, these researchers constructed the multi-degree of freedom (MDOF) models of 3 bridges and 2 reinforced-concrete buildings using a FE based package-program. Then, these numerical models are converted from MDOF to representative or equivalent single-degree of freedom (ESDOF) systems. Consequently, the extensive computational time and effort regarding to the time history dynamic analyses for each MC simulation of MDOF systems have been reduced. Then, one can construct the equivalent fragility curves using the ESDOF, instead of the MDOF system of structures. However, the limitation of these conversions may also cause non-negligible errors for the analytical fragility curves [29].

This study presents a new theoretical methodology (ALFA) to reduce the computational time and effort required for an accurate analytical fragility analysis. To the best of the author's knowledge, an accurate analytical fragility analysis utilizing the parameters of dynamic amplification factor and phase angle regarding to the dynamic characteristics of structures has not been employed. In this methodology, these parameters are calculated using relatively less number of harmonic time history analyses. In other words, to satisfy the desired accuracy for the fragility analysis of a structure requires tens of thousands (e.g., 56000 in [8]) or even hundreds of thousands FE based dynamic time history analyses, which is called a MC based brute-force methodology. For the similar accuracy, ALFA requires a comparatively very few number (a total of 100 dynamic harmonic analyses were used

to calculate the dynamic parameters) of dynamic analyses to construct the fragility curves of linear structural systems. Therefore, the required time for ALFA is significantly less than the MC based brute-force methodology. As a case study, the analytical fragility curves of a total of 70 different multi-degree of freedom (MDOF) mass-column systems are constructed using both the MC based brute-force methodology and ALFA with similar accuracies. Therefore, it was shown that the fragility curves of the MDOF mass-column systems have been accurately (0.23 % mean-error with a standard deviation of 0.29 %) obtained with ALFA 240 times faster than the MC based brute-force methodology.

Overall, this new methodology would be beneficial for (i) the design-regulations of structures to build more sustainable, stable, and safer structures, (ii) the decision on whether the existing structures should be retrofitted, and (iii) the preliminary risk assessment of nonlinear structural systems.

## 2. Material and Method

The presented methodology (ALFA) decreases the computational time and effort required for an accurate analytical linear fragility analysis. ALFA is addressed in five main sub-sections; (1) structural modeling, (2) stochastically generation of wind forces, (3) harmonic analysis for generated wind forces, (4) steady-state deformation response, and (5) probability of exceedance for failure estimation. The flowchart in Figure 1 represents these sub-sections to summarize the presented methodology.

### 2.1. Structural Modeling

A general MDOF system, structurally, consists of several matrices regarding to mass, stiffness and damping. As the case studies for this work, first, these matrices are assigned in a Matlab-code to define a total of 70 different MDOF mass-column systems as in Figure 1. The degree of freedom (DOF) of these 70 different MDOF systems varies from 1 to 200 in increments of 2 (for the range between 1 and 100) and in increments of 5 (for the range between 100 and 200). Thus, the size of the matrices (e.g., mass, damping, stiffness) of each mass-column system varies regarding to the number of the DOF. For example, 2DOF and 4DOF systems have two lumped masses and two columns, and four lumped masses and four columns, respectively. After defining the MDOF systems, second, the assumption of Panofsky and Dutton [36] was used in order to define the excitation forces for the MDOF systems. According to this assumption, wind-speed ( $V(z,t)$ ) varies with the ratio of  $z$  (height above ground in [m]) to  $h$  (the reference height=10 m) as in Eq.1. From fluid dynamics, the applicable wind-force ( $F(z,t)$ ) in time domain depends on square of the wind-speed, as follows (see [8]);

$$F(z,t) = \frac{\rho_{\text{air}} A C_d}{2} [V(z,t)]^2, \quad \text{where} \quad V(z,t) = V(t)_h \left[ \frac{z}{h} \right]^{(1/7)} \quad (1)$$

in which  $A$  is frontal area [m<sup>2</sup>],  $\rho_{\text{air}}$  is air density [kg/m<sup>3</sup>],  $C_d$  is non-dimensional drag coefficient, and  $V(t)_h$  is a function of wind-speed [m/s] in terms of time at the reference height of  $h$ , 10 m.

To capture the characteristics of the dynamic response of the MDOF systems, ALFA utilizes the frequency-response parameters (Rd: dynamic amplification factor, and  $\phi$ : phase angle). The frequency-response parameters of each MDOF system could be obtained using a series of harmonic analyses. Thus, a total of 100 harmonic excitation forces of  $F(z,t,w)$ , which is defined in the equation below, is assigned to each lumped-mass of the MDOF systems as in Figure 1.

$$F(z,t,w) = \frac{\rho_{\text{air}} A C_d}{2} \left[ V(t)_h \left( \frac{z}{h} \right)^{(1/7)} \right]^2 \sin(wt), \quad \text{where} \quad w = [0.05, 0.10, 0.15, \dots, 5.00] \quad (2)$$

in which the square term represents the amplitude of the harmonic excitation forces previously addressed in Eq.1. Each frequency ( $w$ ) of these harmonic excitation forces varies from 0.05 [rad/sec] to 5.00 [rad/sec] in increments of 0.05 [rad/sec].

The frequency-response parameters (Rd and  $\phi$ ) are selected as the primary output of this sub-section. Rd (dots in Figure 2) is the ratio of the maximum displacement of the dynamic response of the MDOF systems subjected to harmonic excitations to the maximum displacement of the static response of the MDOF systems. The maximum static displacement,  $(U_{st})_0$  can be computed using the multiplication of the inverse of the stiffness matrix and the excitation force vector ( $(U_{st})_0 = K^{-1}F$ ). The maximum dynamic displacement can be computed using a numerical integration method or finite element methods. For the case studies of this work, Wilson method was selected as the numerical integration method in order to compute the dynamic response of the MDOF systems, and

consequently to compute  $R_d$  and  $\phi$ .  $\phi$  (stars in Figure 2) is the phase angle which defines the time lag in frequency domain between the computed dynamic response and the applied excitation force.

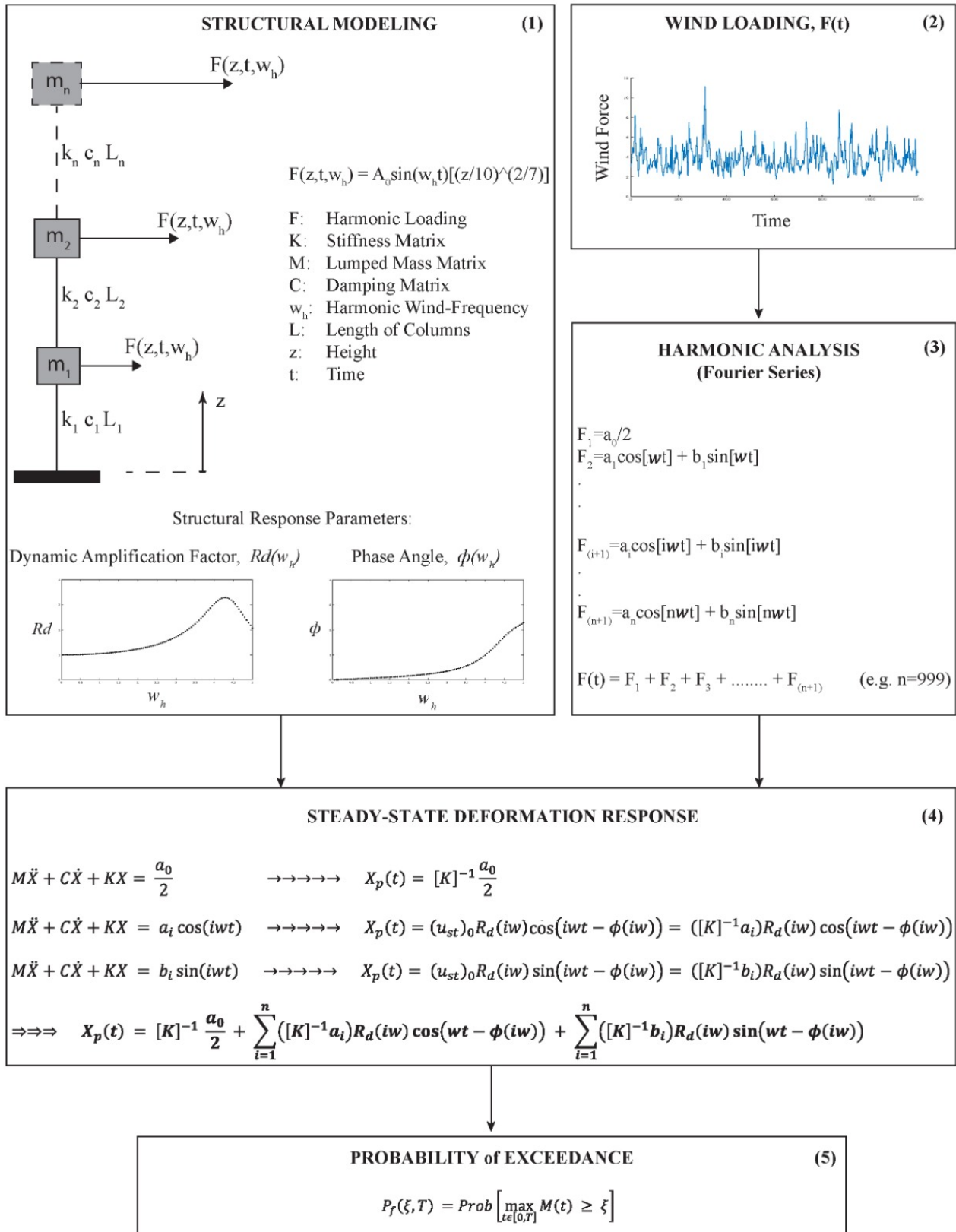
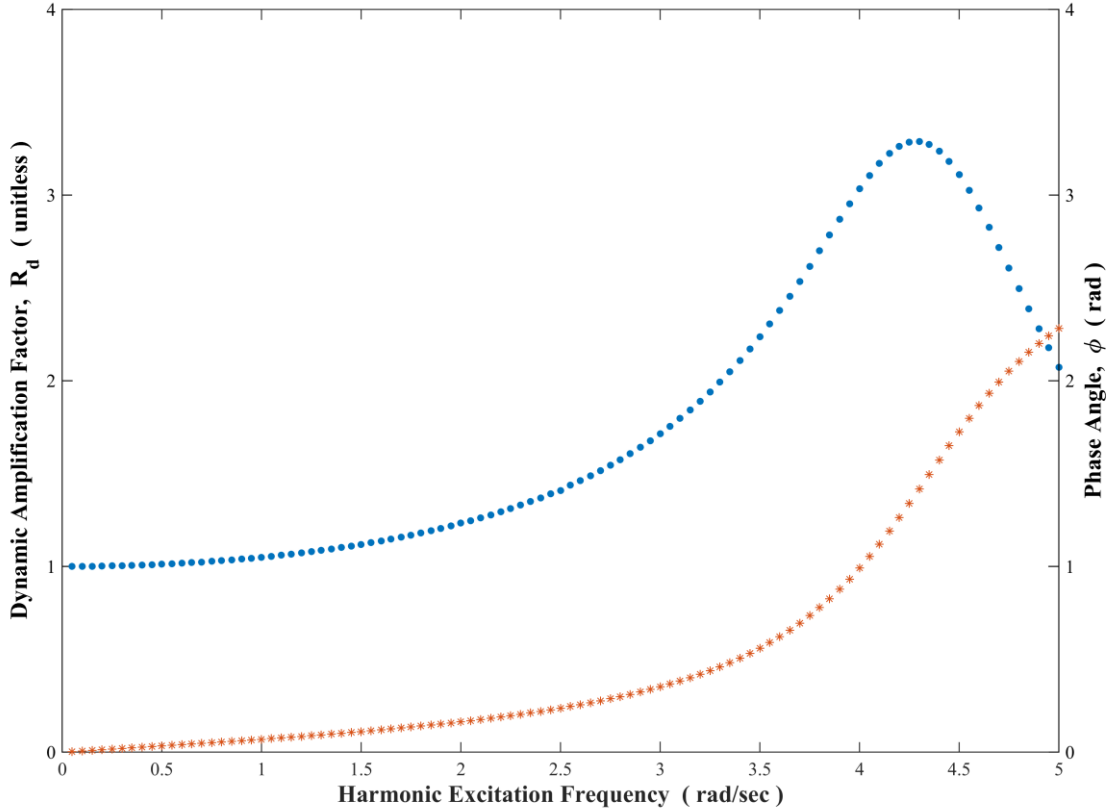


Figure 1. Flowchart for ALFA



**Figure 2.**  $R_d$  (dots) and  $\phi$  (stars) in frequency domain varying from 0.05 rad/sec to 5.00 rad/sec in increments of 0.05 rad/sec for 3-DOF mass-column system

The frequency-response parameters are particularly useful to calculate the dynamic response ( $U_{dyn}$ ) of the MDOF systems subjected to harmonic excitation forces. The equation below can be used for this calculation [37];

$$U_{dyn}(t) = (U_{st})_0 R_d \sin(\omega t - \phi) \quad (3)$$

in which  $(U_{st})_0$  is the maximum static response of the MDOF system as addressed above. Additionally, it should be stated that each of the frequency-response parameters ( $R_d$  and  $\phi$ ) is a function of the harmonic excitation frequency,  $\omega$ . The functions of  $R_d$  and  $\phi$  are plotted in Figure 2 for a 3-DOF system, as an example among a total of 70 different case studies.

In reality, the wind excitation forces are not harmonic; they are in irregular forms and stochastic within varying frequencies in time domain. Thus, first, the stochastic wind-force samples will be generated for the excitation forces of 70 different MDOF systems in Section 2.2. Second, the dynamic response of the MDOF systems subjected to the generated wind-samples will be accurately obtained by Section 2.3 and 2.4.

## 2.2. Stochastically Generated Wind-Force Samples

As mentioned previously, the drag force or wind-force ( $F(z, t, w)$ ) depends on wind-speed (Eq. 1). The critical step for the calculation of the drag force is to have realistic wind-speed samples. Therefore, in order to generate a significant number of realistic wind-speed samples, wind-speed generation process, which was presented by the study of Ciftci et al. [8], is used. According to this generation process, it is necessary to have power spectral density (PSD) regarding to wind-speed measurements. For an empirical formula of PSD, Davenport's formula [38] is used as follows;

$$PSD(\omega) = \frac{\frac{916700}{2\pi} c\omega}{\left[1 + \left(\frac{191\omega}{\mu_V}\right)^2\right]^{(4/3)}} \quad (4)$$

where  $c$  is the surface drag coefficient (selected to be 0.005 for this work based on the recommendation in [38] for an open unobstructed country),  $\omega$  is the wind frequency [rad/sec], and  $\mu V$  is the mean of the wind-speed samples. For a targeted mean wind-speed value, randomly distributed Gaussian wind-speed samples ( $V^G$ ) in time domain can be generated using spectral representation method as follows [39];

$$V^G(t) = \sum_{r=1}^k A_r \sin(\omega_r t) + B_r \cos(\omega_r t) \tag{5}$$

in which  $A_r$  and  $B_r$  are independent Gaussian random variables with zero mean and variance ( $\sigma_r^2$ ), which can be calculated;

$$\sigma_r^2 = PSD(\omega_r)\Delta\omega \tag{6}$$

where  $PSD(\omega_r)$  is the discrete value of the power spectral density at  $\omega_r$ , and  $\Delta\omega$  is the interval of wind frequencies for equally divided frequency range.

Eqs. 4-6 generate the randomly distributed Gaussian wind-speed samples. Since wind samples are commonly represented by Lognormal or Weibull distributions in the literature, the generated Gaussian samples are converted to the Lognormal distribution using Nataf model [40], as described in the study of Ciftci et al. [8]. By the repetition of the steps of the generation process, a total of 1,000 different wind-speed samples were randomly generated for each mean wind-speed (varying from 20 m/s to 32 m/s in increments of 0.5 m/s). As an example for 3DOF system, one of the generated wind-speed samples can be seen in Figure 3 for the targeted mean wind-speed (30 m/s). Furthermore, using this wind-speed sample and Eq. 1 (e.g., arbitrarily selected values of  $A$ ,  $C_d$  and pair are 3 m<sup>2</sup>, 1.0 and again 1.0, respectively), the wind-force sample was also calculated and shown in Figure 3.

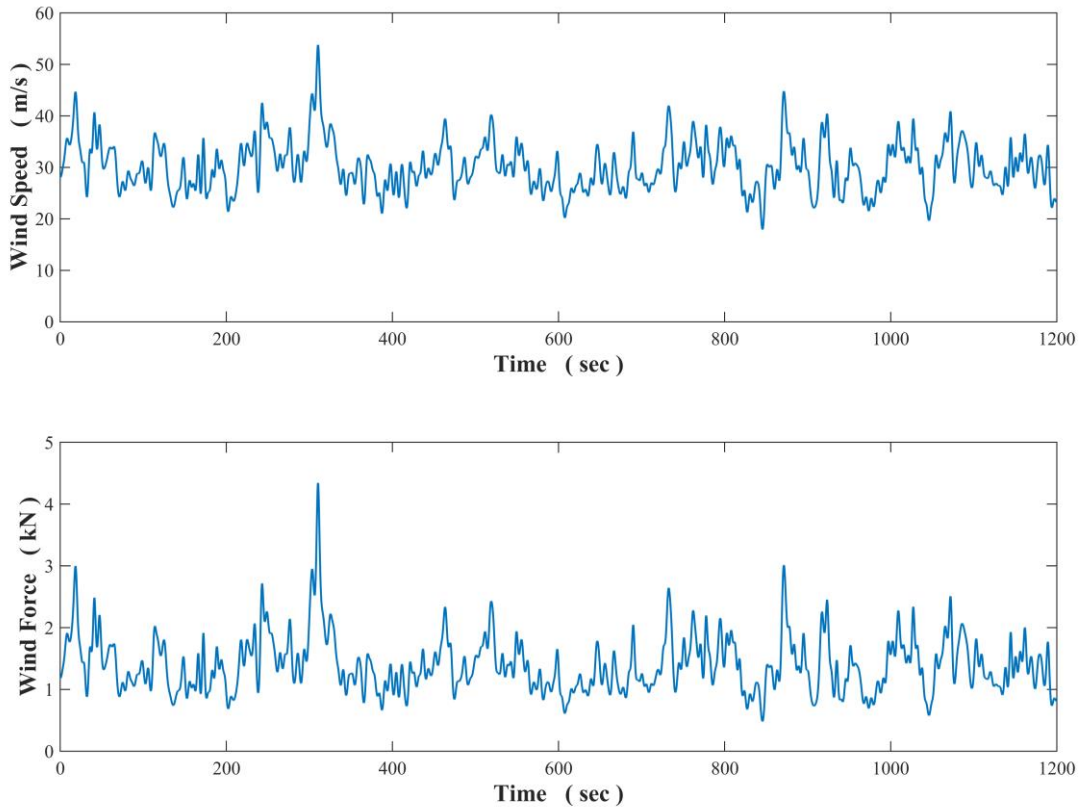


**Figure 3.** One of the generated wind-speed samples for the targeted mean wind-speed, 30 m/s (top); the calculated wind-force sample using the wind-speed sample and Eq. 2 (bottom)

### 2.3. Harmonic Analysis for Generated Wind Forces

Any periodic function can be represented by Fourier series as the summation of an infinite number of sine and cosine terms. The Fourier series representation for the wind-force samples  $[F(t)]$  randomly generated in *Section 2.2* can be written as follows;

$$F(t) = \frac{a_0}{2} + \sum_{n=1}^{n_f} (a_n \cos(n\omega t) + b_n \sin(n\omega t)), \quad \text{where } \omega = \frac{2\pi}{\tau} \quad (7)$$

where  $a_0$ ,  $a_n$  and  $b_n$  are constant coefficients.  $\omega$  and  $\tau$  are the fundamental frequency and the length of the periodic wind-force samples, respectively. For the case study of this research, upper limit of the summation,  $n_f$ , was arbitrarily selected to be 999 to obtain the desired accuracy, and a total of 24,000 generated wind-force samples with varying frequencies for each targeted mean wind-speed (from 20 m/s to 32 m/s in increments of 0.5 m/s) could be represented by the summation of a total of 47,976,000 ( $24000(1 + 999 + 999)$ ) harmonic wind-forces using the Fourier series representation.

### 2.4. Steady-State Deformation Response

In this study, the generated wind-force samples are the excitation loading for the MDOF systems, and these forces can be expanded within a number of Fourier series as described in *Section 2.3*. According to this expansion (Eq. 7), the equation of motion for the linear MDOF systems can be written as follows,

$$M\ddot{X} + C\dot{X} + KX = F(z, t) = \left( \frac{a_0}{2} + \sum_{n=1}^{999} (a_n \cos(n\omega t) + b_n \sin(n\omega t)) \right) \left( \left( \frac{z}{h = 10} \right)^{(2/7)} \right) \quad (8)$$

in which  $h$  is the height above ground, and  $z$  is the location-vector for the lumped masses of the MDOF systems, as previously addressed. Furthermore,  $M$ ,  $C$ , and  $K$ , which have been defined in *Section 2.1*, are the mass, damping, and stiffness matrices of the systems, respectively.  $X$  is the displacement-vector for the MDOF systems,  $\omega$  is the fundamental frequency of the periodic wind-force samples as in Eq. 7, and the other variables have been also defined previously.

Using the principle of superposition and knowing that both  $R_d$  and  $\phi$  are a function of  $n$  times  $\omega$  ( $n\omega = w$  defined in *Section 2.1*), the steady-state solution of the equation of motion (Eq. 8) can be represented as the summation of the steady-state solutions of each equation as follows;

$$M\ddot{X} + C\dot{X} + KX = (a_n \cos(n\omega t)) \left( \left( \frac{z}{h} \right)^{(2/7)} \right) \quad (9)$$

$$\begin{aligned} \text{from Eq. 3 } \Rightarrow \vec{X}_p(t) &= (u_{st})_0 R_d(n\omega) \cos(n\omega t - \phi(n\omega)) \\ \Rightarrow \vec{X}_p(t) &= ([K]^{-1} a_n) R_d(n\omega) \cos(n\omega t - \phi(n\omega)) \end{aligned}$$

$$M\ddot{X} + C\dot{X} + KX = (b_n \sin(n\omega t)) \left( \left( \frac{z}{h} \right)^{(2/7)} \right) \quad (10)$$

$$\begin{aligned} \text{from Eq. 3 } \Rightarrow \vec{X}_p(t) &= (u_{st})_0 R_d(n\omega) \sin(n\omega t - \phi(n\omega)) \\ \Rightarrow \vec{X}_p(t) &= ([K]^{-1} a_n) R_d(n\omega) \sin(n\omega t - \phi(n\omega)) \end{aligned}$$

$$\begin{aligned} M\ddot{X} + C\dot{X} + KX &= \left( \frac{a_0}{2} \right) \left( \left( \frac{z}{h} \right)^{(2/7)} \right) = \left( \frac{a_0}{2} \right) (\cos(n\omega t)) \left( \left( \frac{z}{h} \right)^{(2/7)} \right), & \text{for } n = 0 \\ \text{from Eq. 3 } \Rightarrow \vec{X}_p(t) &= (u_{st})_0 R_d(n\omega) \cos(n\omega t - \phi(n\omega)), & \text{for } n = 0 \\ \Rightarrow \vec{X}_p(t) &= \left( [K]^{-1} \frac{a_0}{2} \right) \end{aligned} \quad (11)$$

Using the principle of superposition for the solutions of Eqs. 9, 10 and 11, the complete steady-state solution of Eq. 8 can be expressed as;

$$\begin{aligned} \vec{X}_p(t) = & \left( [K]^{-1} \frac{a_0}{2} \right) + \sum_{n=1}^{999} ([K]^{-1} a_n) R_d(n\omega) \cos(n\omega t - \phi(n\omega)) \\ & + \sum_{n=1}^{999} ([K]^{-1} b_n) R_d(n\omega) \sin(n\omega t - \phi(n\omega)) \end{aligned} \quad (12)$$

## 2.5. Probability of Exceedance for Failure Estimation

Fragility analysis requires the comparison between the displacement-demand of the lumped-masses of the MDOF mass-column systems and a predefined certain damage state. As the case studies for this work; while the displacement-demand is calculated using Eq. 12, the certain damage state can be defined as the compressive yield stress (due to the wind-induced bending moment) of the column material for the MDOF systems. Thus, the limit state of the fragility analysis is based on the yield moment ( $M_y$ ) of the base column. After defining the limit state (or threshold,  $\xi$ ), the probability of exceedance for the failure estimation ( $P_f$ ) can be calculated in terms of a given time period of  $T$  ([8]);

$$P_f(\xi, T) = \text{Prob} \left[ \max_{t \in [0, T]} M(t) \geq M_y \right] \quad (13)$$

in which  $M(t)$  is the calculated moments in time domain at the base section of the column when the MDOF systems are subjected to randomly generated wind loading.  $M(t)$  is calculated using the complete steady-state solution ( $\vec{X}_p(t)$ ), expressed in Eq. 12, because  $M(t)$  depends on  $\vec{X}_p(t)$  according to the knowledge of the fixed-end-moments in the text-books of structural analysis. As mentioned previously,  $M_y$  is the threshold for the yield moment during a time interval ( $T$ ). Thus, it can be accepted that the threshold is equal to the yield moment, and it can be expressed as;

$$M_y = \frac{\pi \sigma_y D^3}{32} \quad (14)$$

where it is assumed that the column has a solid cross-section. As the case studies of this work, the yield stress ( $\sigma_y$ ) and the diameter ( $D$ ) of the section of the base column were arbitrarily selected to be 28 MPa for a live wood material and 0.5 m, respectively.

## 3. Results

The main goal of this paper is to present a new, fast, and accurate methodology on constructing analytical fragility curves for linear structural systems. To compare the accuracy and the required computational time of ALFA with the reliable MC based brute force method, the fragility curves of a total of 70 different MDOF systems subjected to a total of 1000 randomly generated wind excitations (regarding to varying wind speeds between 20 m/s to 32 m/s in increments of 0.5 m/s) were computed using both methods. Since the construction of the fragility curve of one MDOF system requires to run a total of 24,000 ( $1,000 \times [32-20] / 0.5$ ) MC simulations for the brute-force method; a total of 1,680,000 ( $24,000 \times 70$ ) MC simulations were run to obtain a total of 70 different fragility curves.

As an example for the case studies in this work, the fragility curves of the 3-DOF system are shown in Figure 4 regarding to the accuracy of ALFA. According to the figure, it is seen that the fragility curves of two different methods are greatly similar. Using the fragility curves of the brute-force method as a base, the maximum of the relative error is 0.90 % throughout the wind-speed axis (from 20 m/sec to 32 m/sec) with a mean of 0.23 % and a standard deviation of 0.29 %. Additionally, when the fragility curves of MDOF systems were separately obtained using the two methods, the required computational times were counted using the Matlab-code, "tic" and "toc" commands. Figure 5 is the plot for the required computational times for two different methodologies versus the number of the degree of freedom (DOF) of structural systems varying from 1 to 200. It can be stated that, according to Figure 5, the difference between the speeds of ALFA and the brute-force method exponentially increases with the number of DOF. Furthermore, it should be noted that all these computational times depend on the speed of CPU and RAM of the authors' computer.

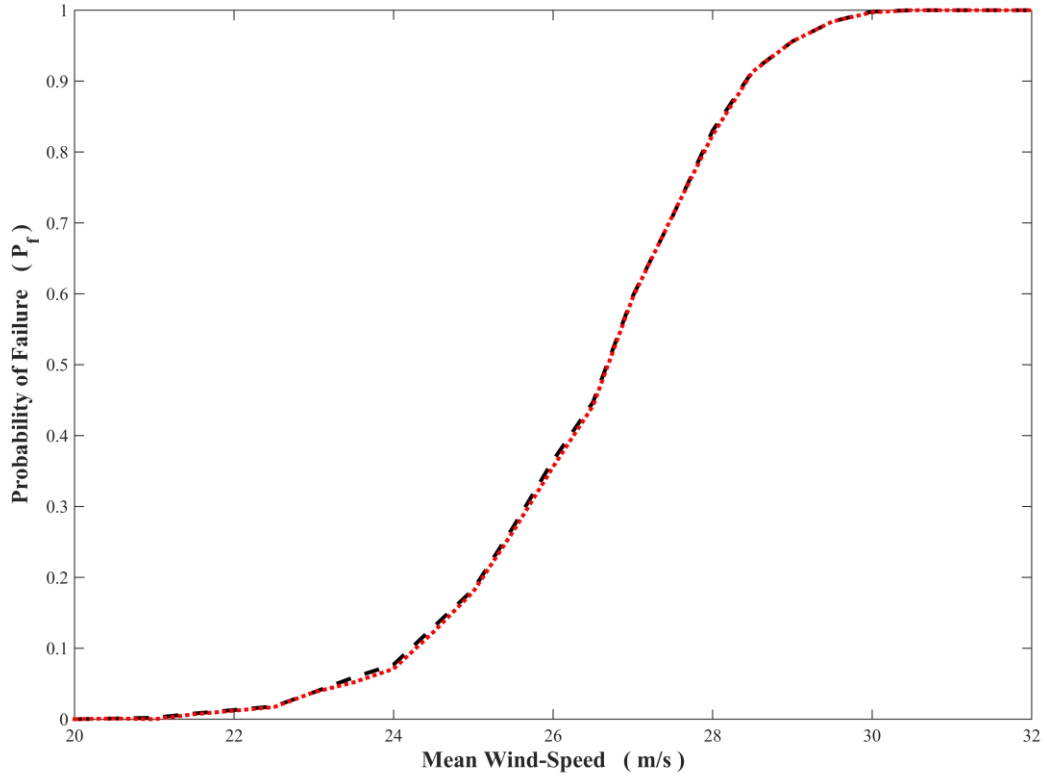


**Figure 4.** The fragility curves of the 3-DOF system using ALFA (dotted line) and MC-based brute-force method (dashed line)

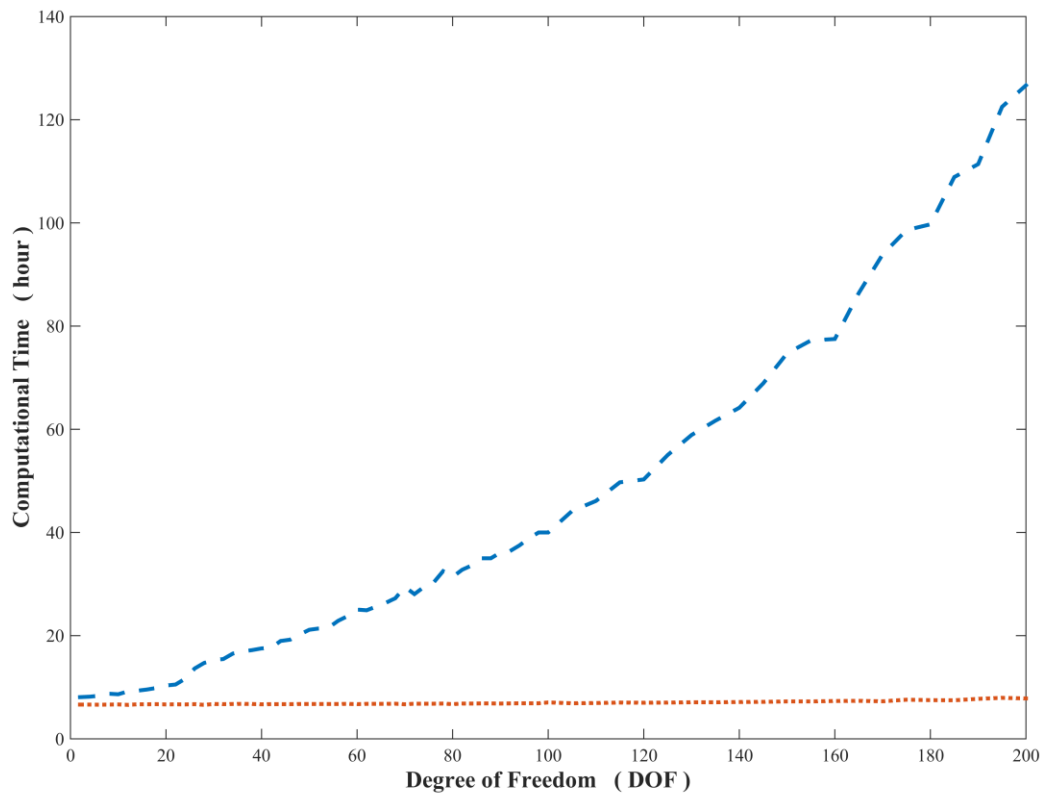


**Figure 5.** The computational time required for ALFA (dotted line) and MC-based brute-force method (dashed line) versus the number of DOF varying from 1 to 200

The required computational time (TALFA) to obtain a fragility curve using ALFA can be also approximately estimated by Eqs. 15-18,

$$T_{ALFA} = T_{sm} + n_{ws}(T_{sgwfs} + T_{hawf} + T_{ssdr}) \quad (15)$$

$$T_{sm} \approx 100(T_{bf}) \quad (16)$$

$$n_{ws}(T_{sgwfs} + T_{hawf} + T_{ssdr}) \approx 0, \quad \text{for a large number of DOF} \quad (17)$$

$$T_{ALFA} \approx T_{sm} \approx 100(T_{bf}), \quad \text{for a large number of DOF} \quad (18)$$

in which  $T_{sm}$ ,  $T_{sgwfs}$ ,  $T_{hawf}$ ,  $T_{ssdr}$  represent the required computational time for the sub-sections (“structural modeling”, “stochastically generated wind-force samples”, “harmonic analysis for generated wind forces”, and “steady-state deformation response”) previously described in Sections 2.1, 2.2, 2.3, and 2.4. The subscripts in Eqs. 15-18 are represented by the initial letters of these sub-sections.  $n_{ws}$  is the number of mean wind-speed for the case studies of this proposed paper ( $n_{ws} = (32-20)/0.5 = 24$  for varying mean wind-speed from 20 m/s to 32 m/s in increments of 0.5 m/s).  $T_{bf}$  is the required computational time of the Wilson method for only one MC simulation. According to Eq. 16, the required computational time for the sub-section (“structural modeling”) of ALFA approximately equal to 100 times  $T_{bf}$ , because Wilson method is also used for ALFA in order to compute the frequency-response parameters ( $R_d$  and  $\phi$ ).  $T_{sgwfs}$ ,  $T_{hawf}$ ,  $T_{ssdr}$  can be accepted negligible, relatively with  $T_{sm}$  (see Eq. 17). Since  $T_{sm}$  is a great value for a large number of DOF, while the other ones ( $T_{sgwfs}$ ,  $T_{hawf}$ ,  $T_{ssdr}$ ) nearly do not depend on the number of DOF. Finally,  $T_{ALFA}$  is approximately equal to 100 times of  $T_{bf}$  (see Eq. 18).

The required computational time ( $T_{bf-m}$ ) to obtain a fragility curve using MC-based brute-force method can be approximately estimated by,

$$T_{bf-m} = n_{ws}n_s T_{bf} \quad (19)$$

in which  $n_s$  (selected as 1,000 for the case studies) is the number of stochastically generated wind-force samples, and  $n_{ws}$  is 24 as previously mentioned. Thus,  $T_{bf-m}$  is approximately equal to 24,000 times  $T_{bf}$ . By assuming that real structures consists of a significant number of structural members, Eq. 18 is compared with Eq. 19 for a large number of the DOF as follows,

$$T_{ALFA} \approx 100 \left( \frac{T_{bf-m}}{n_s n_{ws}} \right) = \left( \frac{T_{bf-m}}{240} \right), \quad \text{when } n_s = 1,000 \ \& \ n_{ws} = 24 \quad (20)$$

From Eq. 20, it can be stated that ALFA is 240 times faster than the other methodology (MC-based brute force) for a large number of DOF. This relationship between  $T_{bf-m}$  and  $T_{ALFA}$  would have been seen in Figure 5, if Figure 5 was plotted for a larger number of DOF than 200.

#### 4. Discussion and Conclusion

This proposed paper presents a new methodology (ALFA) on fast constructing the fragility curves of linear structures with a negligible error. There is a trade-off between the speed and the accuracy of the methodology. If the dynamic amplification factor and phase angle of a structure are obtained using a less number of varying harmonic loading frequency, the speed of ALFA will increase (see Eqs. 16-18). For example, the mean error of the fragility analysis of the 3-DOF mass-column system is 0.23 % (Figure 4), while the number of varying harmonic loading frequency (Eq. 1) is 100 between 0.05 rad/sec and 5.00 rad/sec in increments of 0.05 rad/sec. Thus, the required computational time of ALFA can be decreased using a less number of varying harmonic loading frequency, but the error will increase. Additionally, the error of the fragility analysis also depends on how much the frequency-response parameters ( $R_d$  and  $\phi$ ) can be represented accurately using an optimum range and optimum interval for the harmonic loading frequency in Eq. 1. Thus, a user of ALFA, first, should focus on the smoothness and the reliability of the parameters frequency domain (Figure 2). Furthermore,  $R_d$  and  $\phi$  are plotted in terms of the discretely varying harmonic loading frequencies in increments of 0.05 rad/sec, for the case studies of this work. Then, these plots are assumed to be a continuous function using cubic-interpolation between the discrete values, in order to calculate the  $R_d$  and  $\phi$  in Eq. 12. This interpolation may explain the reason to have an increasing error. The other reason of the error is due to the application of the harmonic analysis on the generated wind-force samples (see Section 2.3). In other words, the harmonic analysis was applied for the case studies of this work using  $n_f = 999$  instead of infinity. If  $n_f$  had been decreased greatly, some non-negligible errors would have occurred.

For a fragility analysis, at least one limit state should be defined. In the literature, for example, the limit states of structures can be separately defined for several performance levels such as immediate occupancy (IO), life safety (LS), and collapse prevention (CP), which are commonly used by civil engineers. The main aim of this paper is to develop a new methodology for fast and accurate fragility analysis of structures, not to compute the fragility curve of a specific structure for a specific performance level. Thus, the performance levels (e.g., IO, LS, and CP) were not used for the case studies of this work. However, it can be stated that ALFA can be applied for MDOF structural systems regarding various performance levels. Additionally, this presented methodology is developed for elastic range of structural materials, not for plastic region. The future investigations about the effects of the geometric and material nonlinearities of structures on ALFA can be also useful, especially, for the nonlinear risk assessment of steel structures.

For the case studies of this work, Wilson method was selected as a numerical integration method to obtain the frequency-response parameters ( $R_d$  and  $\phi$ ), which are addressed in Section 2.1. Whereas Wilson method is one of the commonly used numerical integration methods in vibration analysis; another numerical method (e.g., Newmark method) or a finite element method would have been also selected. The accuracy of the presented methodology depends on the accuracy of the Wilson method used for Section 2.1, "structural modeling". Thus, it is greatly important to accurately model the structures using a reliable numerical or finite element method.

For the loading condition in the case studies of this work, Davenport's formula was selected regarding to the power spectral density (PSD) for Section 2.2. Although Davenport's formula is one of the most commonly used empirical formulas, another empirical formula would have been selected for wind-speed generation, or enough number of real wind-speed measurements would have been used.

It is well known that structures before being constructed are often modeled by engineers using finite element methods (FEMs). So, the frequency-response parameters of these structures, which are required for ALFA, can be rapidly computed using the FE models of the structures instead of using numerical integration methods, such as Wilson method. In other words, several harmonic excitation loads in varying frequencies can be applied using the FE models, and the frequency-response parameters corresponding to critical points of the structures can be obtained. Then, the demand response of the structures subjected to random excitation forces can be rapidly computed by using ALFA, without solving dynamic equations anymore. Furthermore, especially for the special structures which have high importance factor for design, the design regulations may be updated in future. In these design regulations, the fragility analysis may be mandatory for these special structures, (i) to build more reliable structures, (ii) to accurately evaluate the insurance of existing structures, and (iii) to decide whether the structures should undergo retrofitting or which kind of repairing strategies and priorities should be applied.

ALFA was developed in this paper in order to accurately simplify and expedite the analytical fragility analysis for the assessment of linear structural systems subjected to wind loading. The main parts of ALFA are (1) to obtain the frequency-response parameters belonging to the dynamic model of structures, (2) to stochastically generate wind-force samples, (3) to represent these wind-force samples using Fourier series, (4) to estimate the steady-state response of the structural systems, and (5) to compute the probability of exceedance of the systems regarding the yield moment capacities of the structural systems. All these steps of ALFA are put into practice as the case studies of this work. The fragility analysis of a total of 70 different MDOF mass-column systems is computed using ALFA and MC based brute-force method to compare the computational time and effort required for both of the methods. This comparison shows that fragility analysis can be computed 240 times faster using ALFA than the latter method.

In summary, ALFA is a powerful tool to rapidly obtain the fragility curves of linear structural systems with a high accuracy level. These fragility curves can provide additional ideas and reliable information on risk assessment of structural design of new buildings for engineers and also on the insurance evaluation of the existing structures for the decisions of policy makers.

## Acknowledgment

The author of this paper would like to express his appreciation to Dr. Hatice Sinem Sas for her help on proofreading for the draft of the paper.

## References

- [1] J.Y. Lee, B.R. Ellingwood, A decision model for intergenerational life-cycle risk assessment of civil infrastructure exposed to hurricanes under climate change, *Reliab. Eng. Syst. Saf.* 159 (2017) 100–107. doi:10.1016/j.res.2016.10.022.

- [2] M.O. Amini, J.W. van de Lindt, Quantitative Insight into Rational Tornado Design Wind Speeds for Residential Wood-Frame Structures Using Fragility Approach, *J. Struct. Eng.* 140 (2014) 1–15. doi:10.1061/(asce)st.1943-541x.0000914.
- [3] S. Cao, J. Wang, Statistical Summary and Case Studies of Strong Wind Damage in China, *J. Disaster Res.* 8 (2013) 1096–1102.
- [4] K. Lee, D. Rosowsky, Synthetic hurricane wind speed records: development of a database for hazard analyses and risk studies, *Nat. Hazards Rev.* (2007) 1–30. doi:10.1061/(ASCE)1527-6988(2007)8:2(23).
- [5] M.G. Stewart, Cyclone damage and temporal changes to building vulnerability and economic risks for residential construction, *J. Wind Eng. Ind. Aerodyn.* 91 (2003) 671–691. doi:10.1016/S0167-6105(02)00462-2.
- [6] J. Shanmugasundaram, S. Arunachalam, S. Gomathinayagam, N. Lakshmanan, P. Harikrishna, Cyclone damage to buildings and structures - a case study, in: *J. Wind Eng. Ind. Aerodyn.*, 2000: pp. 369–380. doi:10.1016/S0167-6105(99)00114-2.
- [7] B. Gardiner, P. Berry, B. Moulia, Review: Wind impacts on plant growth, mechanics and damage, *Plant Sci.* 245 (2016) 94–118. doi:10.1016/j.plantsci.2016.01.006.
- [8] C. Ciftci, S.R. Arwade, B. Kane, S.F. Brena, Analysis of the probability of failure for open-grown trees during wind storms, *Probabilistic Eng. Mech.* 37 (2014) 41–50. doi:10.1016/j.probenmech.2014.04.002.
- [9] A.C. Khanduri, G.C. Morrow, Vulnerability of buildings to windstorms and insurance loss estimation, *J. Wind Eng. Ind. Aerodyn.* 91 (2003) 455–467. doi:10.1016/S0167-6105(02)00408-7.
- [10] T.W. Schmidlin, Human fatalities from wind-related tree failures in the United States, 1995-2007, *Nat. Hazards.* 50 (2009) 13–25. doi:10.1007/s11069-008-9314-7.
- [11] D.O. Prevatt, J.W. van de Lindt, E.W. Back, A.J. Graettinger, S. Pei, W. Coulbourne, R. Gupta, J. Darryl, A. Duzgun, Making the Case for Improved Structural Design: Tornado Outbreaks of 2011, *Leadersh. Manag. Eng.* 12 (2012) 254–270.
- [12] Y. Tamura, Wind-Induced Damage To Building and Disaster Risk Reduction, in: *17th Asia-Pacific Conf. Wind Eng.*, Taipei, Taiwan, 2009.
- [13] K.H. Lee, D. V. Rosowsky, Fragility assessment for roof sheathing failure in high wind regions, *Eng. Struct.* 27 (2005) 857–868. doi:10.1016/j.engstruct.2004.12.017.
- [14] J.W. van de Lindt, T.N. Dao, Performance-Based Wind Engineering for Wood-Frame Buildings, *J. Struct. Eng.* 135 (2009) 169–177. doi:10.1061/(ASCE)0733-9445(2009)135:2(169).
- [15] A. Quilligan, A. O'Connor, V. Pakrashi, Fragility analysis of steel and concrete wind turbine towers, *Eng. Struct.* 36 (2012) 270–282. doi:10.1016/j.engstruct.2011.12.013.
- [16] V. Sim, W.Y. Jung, Comparison of Wind Fragility for Window System in the Simplified 10 and 15-Story Building Considering Exposure Category, *World Acad. Sci. Eng. Technol.* 10 (2016) 1627–1641.
- [17] J.R. McDonald, K.C. Mehta, J.E. Minor, Tornado-resistant design of nuclear power-plant structures, *Nucl. Saf.* 15 (1974) 432–439.
- [18] R.P. Kennedy, C.A. Cornell, R.D. Campbell, S. Kaplan, H.F. Perla, PROBABILISTIC SEISMIC SAFETY STUDY OF AN EXISTING NUCLEAR POWER PLANT., *Nucl. Eng. Des.* 59 (1980) 315–338. doi:10.1016/0029-5493(80)90203-4.
- [19] S. Kaplan, H.F. Perla, D.C. Bley, A Methodology for Seismic Risk Analysis of Nuclear Power Plants, *Risk Anal.* 3 (1983) 169–180. doi:10.1111/j.1539-6924.1983.tb00118.x.
- [20] G.C. Marano, R. Greco, M. Mezzina, Stochastic approach for analytical fragility curves, *KSCE J. Civ. Eng.* 12 (2008) 305–312. doi:10.1007/s12205-008-0305-8.
- [21] J.W. Van de Lindt, D. V Rosowsky, Strength-based reliability of wood shearwalls subject to wind load, *J. Struct. Eng.* 131 (2005) 359–363. doi:10.1061/(Asce)0733-9445(2005)131:2(359).

- [22] B.R. Ellingwood, D. V Rosowsky, Y. Li, J.H. Kim, Fragility Assessment of Light-Frame Wood Construction Subjected to Wind and Earthquake Hazards, *J. Struct. Eng.* 130 (2004) 1921–1930. doi:10.1061/(ASCE)0733-9445(2004)130:12(1921).
- [23] D. V. Rosowsky, B.R. Ellingwood, Performance-Based Engineering of Wood Frame Housing: Fragility Analysis Methodology, *J. Struct. Eng.* 128 (2002) 32–38. doi:10.1061/(ASCE)0733-9445(2002)128:1(32).
- [24] A. Singhal, A.S. Kiremidjian, Method for Probabilistic Evaluation of Seismic Structural Damage, *J. Struct. Eng.* 122 (1996) 1459–1467. doi:10.1061/(ASCE)0733-9445(1996)122:12(1459).
- [25] Y. Pan, A.K. Agrawal, M. Ghosn, Seismic fragility of continuous steel highway bridges in New York state, *J. Bridg. Eng.* 12 (2007) 689–699. doi:10.1061/(ASCE)1084-0702(2007)12:6(689).
- [26] D. Karmakar, S. Ray-Chaudhuri, M. Shinozuka, Finite element model development, validation and probabilistic seismic performance evaluation of Vincent Thomas suspension bridge, *Struct. Infrastruct. Eng.* 11 (2015) 223–237. doi:10.1080/15732479.2013.863360.
- [27] B. Sun, Y. Zhang, D. Dai, L. Wang, J. Ou, Seismic fragility analysis of a large-scale frame structure with local nonlinearities using an efficient reduced-order Newton-Raphson method, *Soil Dyn. Earthq. Eng.* 164 (2023) 107559.
- [28] W.-S. Yun, H.J. Ham, H.-J. Kim, S. Lee, Evaluation of Extreme Wind Fragility of Balcony Window Systems in Apartments, *J. Archit. Inst. Korea Struct. Constr.* 31 (2015) 3–11.
- [29] M. Rota, A. Penna, C.L. Strobbia, Processing Italian damage data to derive typological fragility curves, *Soil Dyn. Earthq. Eng.* 28 (2008) 933–947. doi:10.1016/j.soildyn.2007.10.010.
- [30] P. Gehl, J. Douglas, D.M. Seyedi, Influence of the Number of Dynamic Analyses on the Accuracy of Structural Response Estimates, *Earthq. Spectra.* 31 (2013) 97–113. doi:10.1193/102912EQS320M.
- [31] S.H. Jeong, A.S. Elnashai, Probabilistic fragility analysis parameterized by fundamental response quantities, *Eng. Struct.* 29 (2007) 1238–1251. doi:10.1016/j.engstruct.2006.06.026.
- [32] M. Shinozuka, M.Q. Feng, J. Lee, T. Naganuma, Statistical Analysis of Fragility Curves, *J. Eng. Mech.* 126 (2000) 1224–1231. doi:10.1061/(ASCE)0733-9399(2000)126:12(1224).
- [33] K.R. Karim, F. Yamazaki, A simplified method of constructing fragility curves for highway bridges, *Earthq. Eng. Struct. Dyn.* 32 (2003) 1603–1626. doi:10.1002/eqe.291.
- [34] D. Straub, A. Der Kiureghian, Improved seismic fragility modeling from empirical data, *Struct. Saf.* 30 (2008) 320–336. doi:10.1016/j.strusafe.2007.05.004.
- [35] M.G. Sfahani, H. Guan, Y.C. Loo, Seismic reliability and risk assessment of structures based on fragility analysis - A review, *Adv. Struct. Eng.* 18 (2015) 1653–1669.
- [36] H.A. Panofsky, J.A. Dutton, *Atmospheric Turbulence: Models and Methods for Engineering Applications*, John Wiley and Sons Ltd, New York, 1984.
- [37] A.K. Chopra, *Dynamics of Structure: Theory and Applications to Earthquake Engineering*, Pearson/Prentice Hall, New Jersey, 2007.
- [38] A.G. Davenport, The spectrum of horizontal gustiness near the ground in high winds, *Q. J. R. Meteorol. Soc.* 87 (1961) 194–211. doi:10.1002/qj.49708737208.
- [39] M. Shinozuka, G. Deodatis, Simulation of Stochastic Processes by Spectral Representation, *Appl. Mech. Rev.* 44(4) (1991) 191–204. doi:10.1115/1.3119501.
- [40] A. Nataf, Détermination des distributions de probabilités dont les marges sont données, *Comptes Rendus l'Académie Des Sci.* 225 (1962) 42–43.